Neutrino Fast Flavor Conversions in Neutron-star Post-Merger Accretion Disks

Xinyu Li[1,2], Daniel Siegel[2], arXiv:2103.02616

[1]Canadian Institute for Theoretical Astrophysics
[2]Perimeter Institute

Introduction

Outflows from the accretion disks formed in the merger of two neutron stars or of a neutron star and a stellar-mass black hole have been identified as a major site of rapid neutron-capture (r-process) nucleosynthesis and as the source of 'red' kilonova emission following the first observed neutron-star merger GW170817. We present long-term general-relativistic radiation magnetohydrodynamic simulations of a typical post-merger accretion disk at initial accretion rates of $\dot{M} \sim 1\,M_\odot\,\mathrm{s}^{-1}$ over 400 ms post-merger. We include neutrino radiation transport that accounts for effects of neutrino fast flavor conversions dynamically. **We find ubiquitous flavor oscillations that result in a significantly more neutron-rich outflow, providing lanthanide and 3rd-peak r-process abundances similar to solar abundances.**

Simulation Setup

Our initial data is an equilibrium torus with $M_{t0} = 0.07M_\odot$ around a black hole of mass $M_{\rm BH} = 3M_\odot$ and spin $\chi_{BH} = 0.8$. The torus has electron fraction $Y_e = 0.1$ with a weak poloidal seed magnetic field. The neutrino radiation transport follows the general-relativistic moment formalism by [1] and is implemented via a M1 scheme adapted from [2].
The growth rates ω of the neutrino fast flavor conversion instability are the imaginary part of ϖ solving the dispersion relation [3]

$$\det\left[\varpi g^{\mu\nu} - \sqrt{2}G_F\left(M^{\mu\nu}_{\nu_e} - M^{\mu\nu}_{\bar{\nu}_e}\right)\right] = 0, \qquad (1)$$

where

$$M^{\mu\nu}_s \equiv \frac{1}{(2\pi)^3}\int E^2 \mathrm{d}E\mathrm{d}\Omega\; f_s v^\mu v^\nu \qquad (2)$$

is the two-moment of the neutrino distribution function and s denotes the species. We calculate the maximum growth rate $\omega \equiv \max|\mathrm{Im}(\varpi)|$ among all roots at a given grid point and set flavor equipartion in our M1 scheme if $\omega^{-1} < 10^{-7}$ s.
We compare two simulations with (`FC`) and without fast flavor conversion (`NFC`).

Disk Evolution

After a brief initial relaxation phase, the magneto-rotational instability is initiated to establish a quasi-stationary accretion state. The accretion rate decreases from initially $\sim 1M_\odot$/yr to $> 0.01\,M_\odot\,\mathrm{s}^{-1}$ over the first 400 ms, above the critical threshold $\dot{M}_{\rm ign} \sim 10^{-3}M_\odot\,\mathrm{s}^{-1}$ for weak interactions to become significant. Powerful disk outflows are launched by imbalanced viscous heating at higher latitudes where neutrino cooling becomes energetically subdominant.
Fast flavor conversions emerge above the energy-dependent neutrinospheres in the disk-corona transition where neutrinos start to decouple and stream freely. Such conversions are ubiquitous, rendering essentially all of the disk vicinity into an unstable region with typical instability growth times up to $\omega^{-1} \sim 0.1$ ns. At later times (~ 300 ms), the instability region shrinks overall and expands into the disk as the density in the disk and outflows decreases, with slower growth rates on an increasing timescale $1 - 100$ ns.

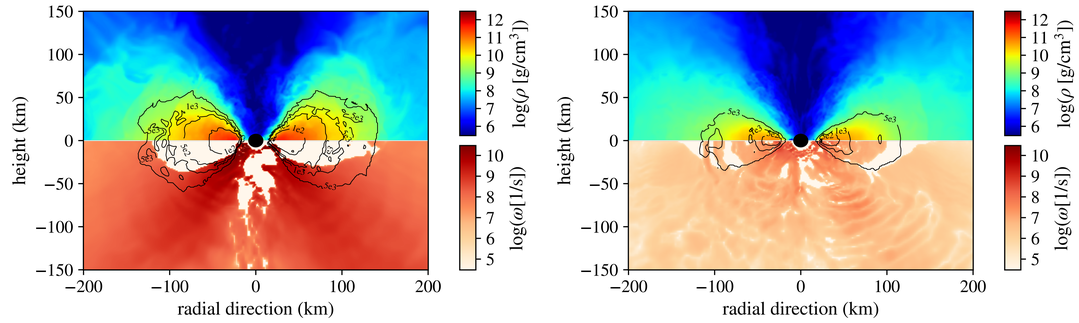

Figure 1: Snapshots of rest-mass density ρ and growth rate ω for fast flavor conversions in the meridional plane at 30 ms (left) and 300 ms (right) for the `FC` run. Contours delineate the mean free path $1/\kappa$ at 100, 500, 1000, 5000 km for $\bar{\nu}_e$ in the energy range of 10–20 MeV.

We find a radially dependent Y_e profile, which translates into a radial lanthanide gradient once the r-process proceeds. This is the result of decreasing neutrino emission from the disk and re-absorption of neutrinos in the outflows as the disk viscously spreads and its midplane density drops over time; the self-regulated inner disk injects increasingly neutron-rich material into the outflows. The radial lanthanide gradient is more pronounced in the absence of fast conversions (`NFC` run), as these suppress the ν_e and $\bar{\nu}_e$ fluxes.

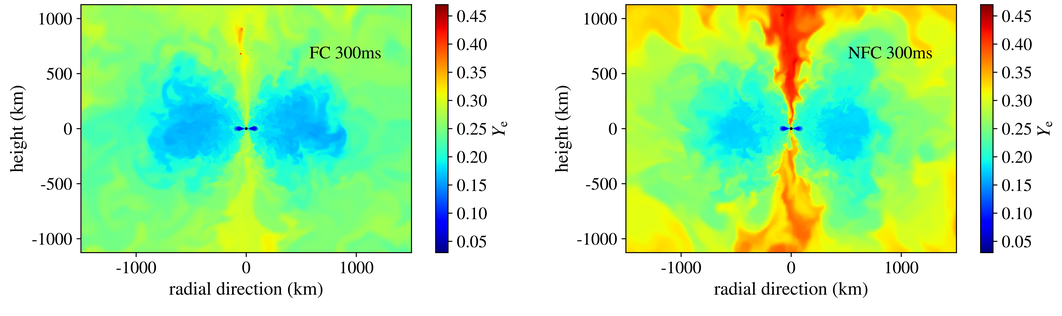

Figure 2: Snapshots of the proton fraction in the meridional plane at 300 ms for the `FC` run (left) and the `NFC` run (right), showing the emergence of an angular and radially dependent composition profile of the outflows. Fast flavor conversions lead to significantly more neutron-rich outflows.

r-process Nucleosynthesis

We trace the outflow with 10^5 passive tracer particles initially placed in the disk. Unbound trajectories of tracers that have reached a distance > 700 km by the end of the simulations are employed as input to nuclear reaction network calculations with `SkyNet` [4] to determine the resulting r-process abundances. The instability decreases the flux of ν_e and $\bar{\nu}_e$ due to mixing into the other less luminous flavors and thus reduce the overall Y_e. The final r-process abundances show strongly enhanced lanthanide and beyond-2nd-peak mass fractions in the presence of fast conversions, in broad agreement with solar abundances.

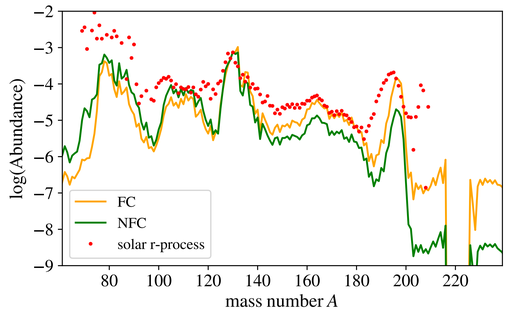

Figure 3: Final nucleosynthetic abundances at 10^9 s from reaction network calculations for the `FC` and `NFC` runs, compared to solar abundances.

`SkyNet` run	$X_{\rm 2nd}$	$X_{\rm 3rd}$	$X_{\rm La}$
`FC`	0.631	0.134	0.097
`NFC`	0.709	0.023	0.049
solar r-process	0.347	0.183	0.139

Table 1: Mass fractions of the 2nd ($125 \le A \le 135$) and 3rd ($186 \le A \le 203$) r-process peak as well as of lathanides with and without accounting for fast conversions.

References

[1] Shibata et al., Prog. of Theor. Phys. 125, 1255 (2011)
[2] Roberts et al. ApJ 831, 98 (2016)
[3] Izaguirre et al., PRL 118, 021101 (2017)
[4] Lippuner and Roberts, ApJS 233, 18 (2017)